Publications of the Astronomical Society of Australia (PASA), Vol. 32, e003, 12 pages (2015).

doi:10.1017/pasa.2015.2

Emission-Line Fluxes of Northern Planetary Nebulae

N. Aksaker[1,4], S. K. Yerli[2], Ü Kızıloğlu[2] and B. Atalay[3]

[1]Vocational School of Technical Sciences, University of Çukurova, Adana, Turkey
[2]Department of Physics, Orta Doğu Teknik Üniversitesi, Ankara, Turkey
[3]Faculty of Science, Department of Physics, Atatürk University, Erzurum, Turkey
[4]Email: naksaker@cu.edu.tr

(Received August 19, 2014; Accepted January 13, 2015)

Abstract

We present long slit spectrophotometric emission line fluxes of bright and extended (<5 arcsec in diameter) planetary nebulae (PNe), selected from a catalogue with suitable equatorial coordinates for northern hemisphere. In total, 17 planetary nebulae have been chosen and observed in 2008–2010. To measure absolute fluxes, broad slit sizes, ranging from 3.5 to 7.5 arcsec were used and thus equivalent widths (EW) of all observable emission line fluxes were also calculated. Among 17 planetary nebulae observed, line flux measurements of 12 of them were made for the first time. This work also aims to extend the sky coverage of emission line flux standards in northern hemisphere (52 planetary nebulae in southern hemisphere; 6 planetary nebulae in northern hemisphere). Electron temperatures and densities, and chemical abundances of these planetary nebulae were also calculated in this work. These data are expected to lead the photometric or spectrometric further work for absolute emission line flux measurements needed for H II regions, supernova remnants etc.

Keywords: planetary nebulae: general, techniques: spectroscopic

1 INTRODUCTION

Studying the stellar evolution in terms of chromospheric activities and kinematics of stars themselves within the Galaxy could also impact on what we know about planetary nebulae (PNe) i.e. when the star's interiors are completely revealed with enriched matter content which will be fed to interstellar medium (ISM) with stellar wind, and therefore enriching the ISM. The key point in these studies lie in the spectroscopic observations of PNe when accurate emission line fluxes are measured (Madsen et al. 2006). Moreover, with the help of this knowledge we can understand how these regions are related to the general structure of the ISM.

In the past, there were several works that they have relied on standard star observations using broad band photometry or spectrophotometry, or even using photon counting detectors. However, these observations help little in improving the emission line flux standards of PNe, H II regions, cataclysmic variables, supernova remnants, etc. (Wright, Corradi, & Perinotto 2005). For photon counting coupled with interference filters: Liller (1955) and O'Dell (1963) had several large error sources such as unknown central wavelength of transmission curves, temperature variations, filter age, and misalignment of various optical components. For broad band photometry (Johnson & Harris 1954; Landolt 1992) and spectrophotometry: (Stone & Baldwin 1983; Massey et al. 1988; Oke 1990); even though there are many types of standard stars available, the flux standards of emission lines are still not adequate in number. In addition to this, several emission and absorption lines coincide in continuum standards (e.g. Balmer series) and when narrow band filters are used, exact contribution of the line fluxes would be difficult. Contrary to abovementioned observation methods, using low read-out noise and high quantum efficiency Charge Coupled Devices (CCDs), spectrophotometry of emission lines of PNe's could very accurately be measured even for faint sources.

Therefore, high precision photometric studies of the emission line fluxes of ionised nebulae are needed.

Lately, Dopita & Hua 1997 (hereafter D97) made slitless spectrophotometric observation of southern compact PNe chosen from the catalogue of Acker et al. 1992 (hereafter A92). They gave Hα, Hβ, O III and laboratory wavelengths of N II and S II emission lines for 39 PNe. For northern hemisphere sources, Wright et al. 2005 (hereafter W05) presented all emission lines of only 6 PNe using similar techniques. Although this was off to a good start, it is not sufficient for northern hemisphere.

Table 1. Journal of observations for the target list. Description of the columns are as follow. The most common object names (Column 1), source coordinates (Column 2 and 3), R magnitude of the source given in SIMBAD (Column 4), source diameter in arcsec (Column 5) given in A92 catalogue, total exposure for blue and red grism (Column 6) and observation date (Column 7).

Object name	α_{2000} (h m s)	δ_{2000} (d m s)	R Mag.	diameter (arcsec)	exposure (s)	Obs. date
Hu 1-1	00 28 15.44	+55 57 54.48	-	5	3000	2010 Jul. 10
BoBn 1	00 37 16.03	− 13 42 58.60	14.6	3	2400	2008 Nov. 9
M 1-4	03 41 43.37	+52 17 00.54	11.9	4	1800	2010 Jul. 11
M 1-5	05 46 50.01	+24 22 02.80	12	2	2400	2008 Nov. 9
K 3-70	05 58 45.34	+25 18 43.80	13.9	1.8	3600	2008 Nov. 9
M 1-17	07 40 22.20	− 11 32 29.92	12.4	3	1200	2008 Nov. 10
SaSt 2-3	07 48 03.67	− 14 07 40.40	13.1	0	1200	2008 Nov. 10
H 4-1	12 59 27.77	+27 38 10.50	14	2.7	6600	2010 Jul. 11
DdDm 1	16 40 18.15	+38 42 20.00	12.9	0.6	2400	2008 Nov. 9
Na 1	17 12 51.89	− 03 15 59.69	10.9	5	4200	2010 Jul. 10
Vy 1-2	17 54 22.98	+27 59 58.10	12.4	4.6	4200	2010 Jul. 10
M 3-27	18 27 48.26	+14 29 06.10	11.9	1	2100	2010 Jul. 11
NGC 6833	19 49 46.58	+48 57 40.20	11	2	1800	2008 Nov. 10
IC 4997	20 20 08.74	+16 43 53.71	-	1.6	2100	2010 Jul. 11
IC 5117	21 32 30.97	+44 35 47.50	-	1.2	780	2008 Nov. 10
Me 2-2	22 31 43.68	+47 48 03.91	10.8	<5	180	2010 Jul. 11
Vy 2-3	23 22 57.89	+46 53 57.79	12.1	4.2	3600	2010 Jul. 10

Table 2. The error budget of the measurements of all 17 PNe: for all emission lines (first column) and five bright lines of Hα, Hβ, O III, N II and He I (second column).

Object name	Total error (all lines)	Total error (bright lines)
Hu 1-1	0.2%	<0.1%
BoBn 1	0.6%	0.3%
M 1-4	0.4%	0.3%
M 1-5	0.5%	0.2%
K 3-70	0.2%	0.1%
M 1-17	0.1%	<0.1%
SaSt 2-3	<0.1%	<0.1%
H 4-1	0.2%	0.1%
DdDm 1	0.2%	<0.1%
Na 1	0.4%	0.1%
Vy 1-2	0.2%	<0.1%
M 3-27	0.3%	0.2%
NGC 6833	0.3%	<0.1%
IC 4997	0.3%	<0.1%
IC 5117	0.2%	<0.1%
Me 2-2	0.2%	<0.1%
Vy 2-3	0.1%	<0.1%

Table 3. Logarithmic extinction constant c_β, and electron temperatures and densities.

Object	C_β	T_e([O III]) (K)	T_e([N II]) (K)	N_e([S II]) (cm^{-3})
Hu 1-1	1.32	11 300	-	-
BoBn 1	-	12 300	-	-
M 1-4	2.20	-	-	1 100
M 1-5	1.24	-	20 300	-
K 3-70	-	-	12 200	2 100
M 1-17	1.03	-	11 900	4 000
SaSt 2-3	0.40	-	10 000	2 700
H 4-1	0.18	12 200	9 400	500
DdDm 1	-	-	-	2 100
Na 1	0.94	10 500	-	-
Vy 1-2	-	11 700	-	3 700
M 3-27	2.68	-	-	-
NGC 6833	0.04	6 000	29 600	>10 000
IC 4997	0.30	-	15 900	>10 000
IC 5117	1.22	9 900	23 700	>10 000
Me 2-2	0.37	10 500	4 500	1 700
Vy 2-3	0.34	10 400	-	-

By increasing the northern hemisphere sources to 17 with this work, a complete set of emission line standards will be builded up for both hemisphere.

2 OBSERVATIONS

The catalogue of A92 includes 1 142 PNe. Therefore, it is used as the main source of our work. The PNe to be observed were selected according to the following criteria:

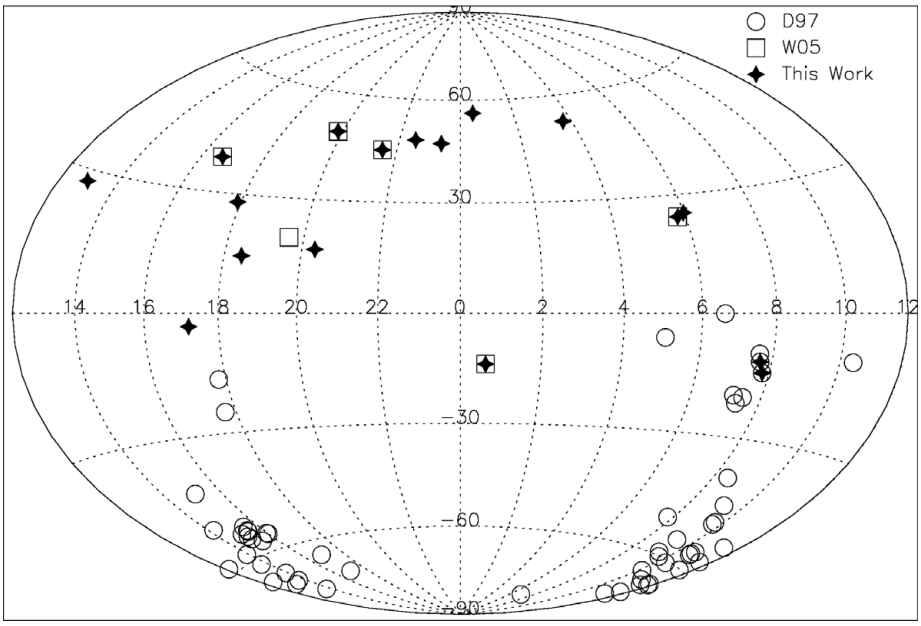

Figure 1. The sky distribution of our target list (stars) in equatorial coordinates. The source of W05 and D97 are represented by squares and circles, respectively.

Table 4. Ionic abundances relative to Hydrogen. All values are scaled with 10^{-6}.

Object	O I	O III	N I	N II	S II	S III	Ar IV
M 1-5	1.28	-	-	5.14	-	-	-
M 1-17	43.8	195	3.08	6.16	-	7.30	-
SaSt 2-3	18.1	1.08	-	13.5	-	-	-
H 4-1	31.7	249	2.15	18.6	6.77	-	-
NGC 6833	0.44	1 770	-	16.2	0.22	0.16	-
IC 4997	-	33.7	-	2.09	-	2.05	0.06
IC 5117	3.06	29.0	-	0.69	0.33	1.21	-
Me 2-2	1.51	216	-	4 550	67.6	318	4.30
Vy 1-2	-	163	-	-	-	-	-

- To select only northern hemisphere PNe, first declination is limited to $\delta > -35^{\circ}$ which reduces the total number to 838.
- Then, RA in between 7^{h} and 12^{h} are excluded from the selection which reduces the total number to 805 PNe.
- From this subset, angular size of PNe smaller than 5 arcsec are selected (i.e. PNe fits to the available slit size). This reduced the total number to 276 PNe.
- Then, less studied 12 PNe were selected.
- 5 PNe which were studied by W05 were added to this subset increasing the total number to 17.

Journal of observations for the selected PNe are given in Table 1.

Sky distribution of target list given in Table 1 is shown in Figure 1. It contains sources of both D97 and W05. It can easily be seen from the figure that our aim of filling sky coverage gaps in northern hemisphere is achieved.

The observations were performed with the TFOSC[1] (TÜBİTAK Faint Object Spectrometer and Camera) coupled with the 150 cm Russian–Turkish Telescope (RTT150). The camera is equipped with a 2048x2048 (15 μm) pixel Fairchild 447BI CCD.

The mean seeing level throughout the observing nights were 1.9 arcsec, ranging from 0.6 to 2.6 arcsec. The seeing measurements were calculated from unfiltered frames by averaging over Full Width at Half Maximum's (FWHM) of field stars which were taken just before the spectrum observations. The seeing characteristics of the site were well determined by Ozisik & Ak (2004).

[1] http://tug.tubitak.gov.tr/tr/teleskoplar/tfosc

Table 5. BoBn 1 fluxes and equivalent widths.

		This work		W05	
Wavelength Å	Ion	log [Flux] (ergs cm^{-2} s^{-1})	log [EW] (Å)	log [Flux] (ergs cm^{-2} s^{-1})	log [EW] (Å)
3 967.41	[NeIII]	-13.680 ± 0.008	2.719 ± 0.240	-	-
4 101.74	Hδ	-13.947 ± 0.020	2.294 ± 0.177	-	-
4 340.47	Hγ	-13.562 ± 0.012	2.656 ± 0.273	-	-
4 363.21	[OIII]	-14.356 ± 0.155	1.507 ± 0.647	-	-
4 387.93	HeI	-14.368 ± 0.014	1.830 ± 0.216	-	-
4 471.68	HeI	-14.195 ± 0.013	2.264 ± 0.066	-	-
4 685.71	HeII	-13.891 ± 0.019	2.124 ± 0.222	-13.103 ± 0.024	2.097 ± 0.107
4 861.20	Hβ	-13.021 ± 0.007	2.917 ± 0.124	-12.425 ± 0.011	2.759 ± 0.128
4 958.52	[OIII]	-12.924 ± 0.006	3.154 ± 0.477	-12.358 ± 0.005	2.797 ± 0.065
5 754.59	[NII]	-	-	-14.447 ± 0.005	1.000 ± 0.105
5 007.57	[OIII]	-12.432 ± 0.001	4.020 ± 0.480	-11.877 ± 0.006	3.188 ± 0.140
5 875.97	HeI	-13.706 ± 0.023	2.316 ± 0.320	-13.278 ± 0.019	2.009 ± 0.255
6 300.30	[OI]	-	-	-14.503 ± 0.069	0.986 ± 0.050
6548.05	[NII]	-13.344 ± 0.716	2.010 ± 0.392	-13.296 ± 0.014	1.674 ± 0.050
6 562.85	Hα	-12.765 ± 0.443	2.226 ± 0.330	-11.934 ± 0.002	2.959 ± 0.045
6 583.45	[NII]	-13.351 ± 0.011	2.449 ± 0.181	-12.828 ± 0.012	2.166 ± 0.059
6 678.15	HeI	-14.504 ± 0.191	1.413 ± 0.400	-13.853 ± 0.022	1.585 ± 0.206
7 065.71	HeI	-	-	-13.723 ± 0.038	1.767 ± 0.109
7 135.80	[ArIII]	-14.161 ± 0.072	1.699 ± 0.354	-	-

Table 6. M 1-5 fluxes and equivalent widths.

		This work		W05	
Wavelength Å	Ion	log [Flux] (ergs cm^{-2} s^{-1})	log [EW] (Å)	log [Flux] (ergs cm^{-2} s^{-1})	log [EW] (Å)
4 101.74	Hδ	-14.201 ± 0.378	1.399 ± 0.817	-	-
4 340.47	Hγ	-14.199 ± 0.000	2.263 ± 0.079	-	-
4 685.71	HeII	-13.681 ± 0.004	2.332 ± 0.207	-	-
4 861.20	Hβ	-13.559 ± 0.004	2.496 ± 0.035	-	-
4 958.52	[OIII]	-13.413 ± 0.002	2.499 ± 0.001	-	-
5 007.57	[OIII]	-12.901 ± 0.001	3.081 ± 0.072	-	-
5 269.20	[KVI]	-14.328 ± 0.009	1.639 ± 0.057	-	-
5 754.59	[NII]	-14.555 ± 0.035	1.385 ± 0.122	-13.355 ± 0.098	1.228 ± 0.102
5 875.97	HeI	-13.960 ± 0.008	1.937 ± 0.064	-12.551 ± 0.007	2.029 ± 0.062
6 300.30	[OI]	-14.795 ± 0.148	1.128 ± 0.332	-13.273 ± 0.032	1.265 ± 0.038
6 312.10	[SIII]	-	-	-13.685 ± 0.034	0.819 ± 0.048
6 548.05	[NII]	-15.115 ± 0.080	0.939 ± 0.118	-12.086 ± 0.002	1.793 ± 0.076
6 562.85	Hα	-12.703 ± 0.013	3.018 ± 0.063	-11.082 ± 0.002	2.817 ± 0.029
6 583.45	[NII]	-13.216 ± 0.018	2.510 ± 0.026	-11.595 ± 0.001	2.498 ± 0.063
6 678.15	HeI	-14.519 ± 0.080	1.273 ± 0.054	-12.940 ± 0.001	1.572 ± 0.032
6 716.47	[SII]	-	-	-13.497 ± 0.005	1.008 ± 0.026
6 730.85	[SII]	-14.730 ± 0.028	1.22 ± 0.058	-13.157 ± 0.001	1.332 ± 0.016
7 065.71	HeI	-14.147 ± 0.004	1.710 ± 0.031	-12.513 ± 0.002	1.942 ± 0.031
7 135.80	[ArIII]	-13.785 ± 0.607	2.115 ± 0.584	-12.530 ± 0.010	1.919 ± 0.045

In the spectroscopic work, mainly G7 (Grism 7: 3 850–6 850 Å; visible), G8 (Grism 8: 5 800–8 300 Å; red) and G14 (Grism 14: 3 275–6 100 Å; blue) were used. The average dispersions were 1.5, 1.1, and 1.4 Å/pixel for G7, G8, and G14, respectively. Considering the telescope optics and seeing conditions, an optimum signal-to-noise ratio (SNR) was reached with the following exposure times: 60 s for *Me 2-2* (a typical bright PNe) and 3600 s for *H 4-1 (*a typical faint PNe). Note that the exposure times were determined according to source's R magnitude given in Table 1.

Each PNe was observed with a slit size which was varied according to the PNe's angular size and seeing: 3.5 arcsec for point-like sources and 7.3 arcsec for wider sources. The

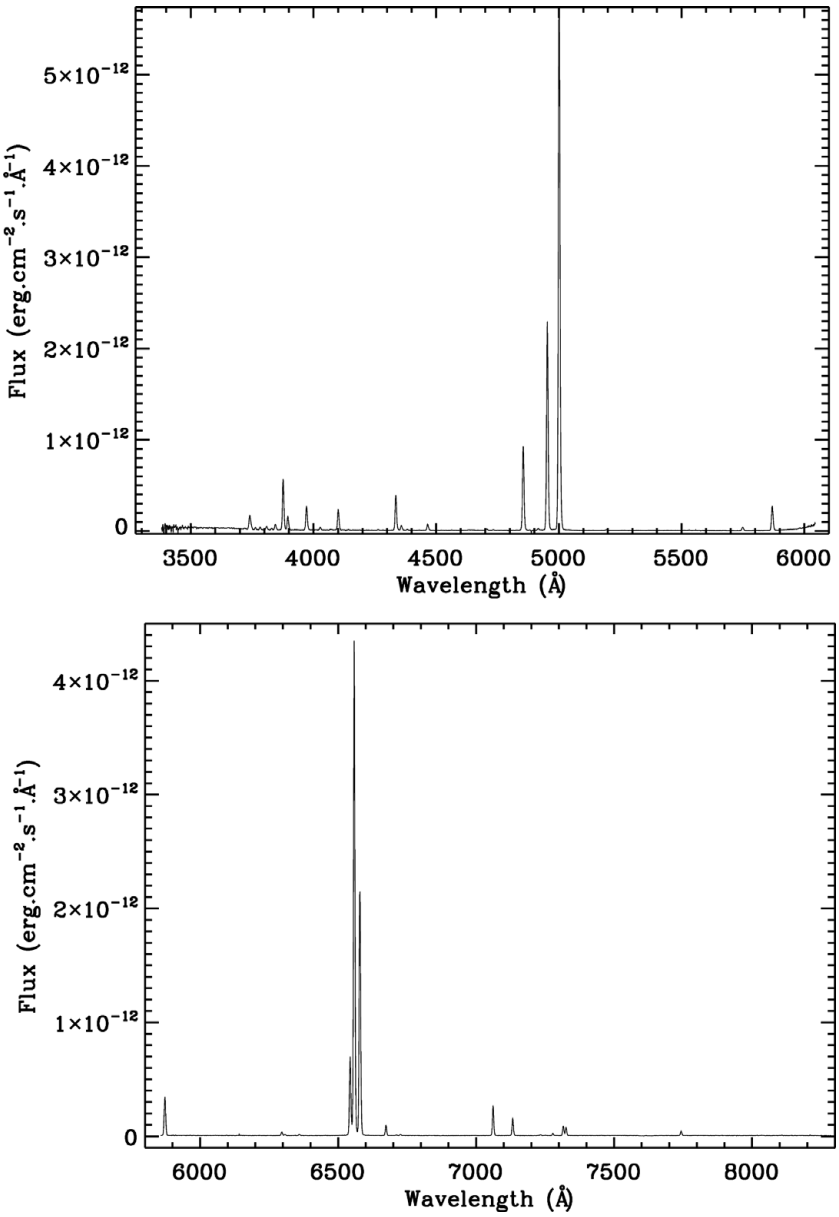

Figure 2. The blue (above panel) and red (below panel) spectra of Me 2-2.

slit position and therefore dispersion axis is aligned to the parallactic angle to avoid loss of light due to the atmospheric refraction. Contrary to work of D97 in southern hemisphere, PNe coordinates in northern hemisphere were quite accurate: Source-to-source pointing accuracy was kept <5 arcsec and there were no loss of frames due to the autoguider failures.

3 DATA ANALYSIS

Headers of TFOSC images were processed using IDL[2] and then they were reduced using standard IRAF[3] tasks e.g. *onedspec* and *image*. The instrumental profile of the sensor was subtracted using standard reduction packages of Image Reduction and Analysis Facility (IRAF). The images were then converted into 1D spectra by using the *apall* task. As for the last stage wavelength and flux calibrations tasks were applied to the spectra.

To achieve a sensible accuracy in the wavelength calibration, different arc lamps were used for different grisms: He+Ne for Grism 7 (hereafter G7); Ne for Grisim 8 (hereafter G8); He for Grism 14 (hereafter G14). Arc lamp atlas of ALFOSC (another spectrograph in FOSC series)[4] were used

[2] http://www.exelisvis.com/language/en-US/ProductsServices/IDL.aspx
[3] IRAF is distributed by the National Optical Astronomy Observatories, which are operated by the Association of Universities for Research in Astronomy, Inc., under cooperative agreement with the National Science Foundation.
[4] http://www.not.iac.es/instruments/alfosc/lamps/

Table 7. NGC 6833 fluxes and equivalent widths.

		This work		W05	
Wavelength Å	Ion	log [Flux] (ergs cm^{-2} s^{-1})	log [EW] (Å)	log [Flux] (ergs cm^{-2} s^{-1})	log [EW] (Å)
3 697.15	H17	-	-	-13.829 ± 0.241	0.000 ± 0.109
3 705.00	He I	-	-	-13.288 ± 0.081	0.423 ± 0.037
3 712.75	He II	–	–	-13.346 ± 0.149	0.401 ± 0.043
3 726.19	[O II]	-	-	-12.259 ± 0.066	1.358 ± 0.012
3 734.37	H13	-	-	-12.977 ± 0.116	0.562 ± 0.024
3 750.15	H12	-	-	-12.920 ± 0.023	0.959 ± 0.004
3 770.63	H11	-	-	-12.812 ± 0.024	1.066 ± 0.005
3 797.90	H10	-	-	-12.689 ± 0.055	1.184 ± 0.003
3 819.70	He I*	-	-	-13.305 ± 0.146	0.573 ± 0.076
3 835.38	H9	-	-	-12.540 ± 0.030	1.334 ± 0.006
3 868.71	[Ne III]	-	-	-11.439 ± 0.020	2.394 ± 0.033
3 889.05	H8	-12.771 ± 0.004	2.219 ± 0.043	-12.142 ± 0.019	1.692 ± 0.024
3 967.41	[Ne III]	-13.889 ± 0.096	1.049 ± 0.159	-11.761 ± 0.001	2.136 ± 0.005
4 026.10	He I*	-12.793 ± 0.011	2.123 ± 0.104	-13.025 ± 0.013	0.905 ± 0.014
4 068.91	C III	-	-	-13.442 ± 0.128	0.481 ± 0.117
4 101.74	Hβ	-	-	-11.954 ± 0.006	1.988 ± 0.001
4 340.47	Hγ	-12.947 ± 0.004	1.788 ± 0.020	-11.673 ± 0.037	2.269 ± 0.026
4 363.21	[O III]	-14.164 ± 0.110	0.567 ± 0.127	-12.247 ± 0.040	1.715 ± 0.056
4 387.93	He I	-	-	-13.601 ± 0.042	0.378 ± 0.006
4 471.68	He I	-	-	-12.613 ± 0.039	1.369 ± 0.030
4 685.71	He II	-13.699 ± 0.070	1.018 ± 0.107	-	-
4 713.38	He I*	-13.727 ± 0.070	0.975 ± 0.107	-13.244 ± 0.009	0.821 ± 0.012
4 724.30	[Ne IV]	-13.884 ± 0.144	0.828 ± 0.188	-	-
4 740.18	[Ar IV]	-	-	-13.447 ± 0.034	0.590 ± 0.039
4 861.20	Hβ	-11.838 ± 0.002	2.827 ± 0.079	-11.315 ± 0.012	2.733 ± 0.033
4 921.93	He I	-13.587 ± 0.095	1.057 ± 0.155	-13.246 ± 0.034	0.785 ± 0.050
4 958.52	[O III]	-11.410 ± 0.001	3.171 ± 0.077	-10.886 ± 0.007	3.003 ± 0.023
5 007.57	[O III]	-11.075 ± 0.000	3.397 ± 0.074	-10.401 ± 0.001	3.439 ± 0.074
5 191.80	[Ar III]	-	-	-14.275 ± 0.177	-0.150 ± 0.186
5 269.20	[K VI]	-13.314 ± 0.024	1.219 ± 0.036	-	-
5 537.89	[C III]	-	-	-13.935 ± 0.082	0.243 ± 0.098
5 754.59	[N II]	-13.314 ± 0.024	1.219 ± 0.036	-13.049 ± 0.047	1.121 ± 0.017
5 875.97	He I	-12.423 ± 0.001	2.129 ± 0.011	-12.038 ± 0.002	2.112 ± 0.011
6 300.30	[O I]	-13.187 ± 0.023	1.524 ± 0.079	-12.841 ± 0.268	1.342 ± 0.272
6 312.10	[S III]	-13.671 ± 0.037	1.113 ± 0.068	-	-
6 363.77	[O I]	-13.622 ± 0.044	1.122 ± 0.051	-13.245 ± 0.006	0.966 ± 0.080
6 548.05	[N II]	-12.723 ± 0.030	1.870 ± 0.010	-12.262 ± 0.007	1.247 ± 0.038
6 562.85	Hα	-11.371 ± 0.001	3.320 ± 0.144	-10.752 ± 0.001	2.838 ± 0.051
6 583.45	[N II]	-12.239 ± 0.001	2.367 ± 0.013	-11.865 ± 0.003	1.867 ± 0.021
6 678.15	He I	-13.048 ± 0.002	1.661 ± 0.010	-12.620 ± 0.007	1.598 ± 0.028
6 716.47	[S II]	-14.203 ± 0.075	0.533 ± 0.189	-13.888 ± 0.033	0.329 ± 0.035
6 730.85	[S II]	-13.897 ± 0.111	0.864 ± 0.074	-13.531 ± 0.029	0.700 ± 0.001
7 065.71	He I	-12.572 ± 0.001	2.170 ± 0.011	-12.130 ± 0.003	2.123 ± 0.009
7 135.80	[ArIII]	-12.547 ± 0.005	2.151 ± 0.067	-	-

to identify the lines in the spectra. The resultant accuracy of wavelength calibration was around ± 1 Å. The reference wavelength used in flux measurements are given in Tables 5–21.

Fluxes of spectrophotometric standards listed in Stone & Baldwin (1983), Baldwin & Stone (1984), Massey et al. (1988), and Oke (1990) were used in flux calibration of all PNe. The standard stars have to be identified both in one of the abovementioned catalogues and in IRAF's repository of standard stars; then the closest one to the target PNe was chosen to eliminate the effect of airmass. Finally, flux calibration tasks of IRAF (*standards*, *sensitivity*, and *calibrate*) applied to PNe images.

A typical reduced pair (red and blue) of spectra are shown in Figure 2. The bright lines in red spectrum are N II λ6 548.05, Hα λ6 582.85, and N II λ6 583.45, and

Table 8. IC 5117 fluxes and equivalent widths.

		This work		W05	
Wavelength Å	Ion	log [Flux] (ergs cm^{-2} s^{-1})	log [EW] (Å)	log [Flux] (ergs cm^{-2} s^{-1})	log [EW] (Å)
3 705.00	HeI	-	-	-13.661 ± 0.155	0.810 ± 0.211
3 712.75	HeII	-	-	-13.656 ± 0.032	0.806 ± 0.122
3 726.19	[OII]	-	-	-12.337 ± 0.004	1.768 ± 0.023
3 734.37	H13	-	-	-13.340 ± 0.088	0.493 ± 0.261
3 750.15	H12	-	-	-13.254 ± 0.021	1.217 ± 0.179
3 770.63	H11	-	-	-13.156 ± 0.053	1.502 ± 0.051
3 797.90	H10	-	-	-13.014 ± 0.005	1.651 ± 0.175
3 819.70	HeI*	-	-	-13.700 ± 0.001	0.846 ± 0.019
3 835.38	H9	-	-	-12.836 ± 0.015	1.767 ± 0.016
3 868.71	[NeIII]	-	-	-11.503 ± 0.002	2.871 ± 0.071
3 889.05	H8	-	-	-12.482 ± 0.013	1.955 ± 0.098
3 967.41	[NeIII]	-	-	-11.844 ± 0.003	2.781 ± 0.100
4 068.91	CIII	-	-	-12.991 ± 0.002	1.382 ± 0.063
4 101.74	Hδ	-12.943 ± 0.214	2.696 ± 0.214	-12.179 ± 0.012	2.387 ± 0.134
4 340.47	Hγ	-12.537 ± 0.388	2.845 ± 0.388	-11.876 ± 0.003	2.581 ± 0.112
4 363.21	[OIII]	-12.832 ± 0.328	2.752 ± 0.328	-12.191 ± 0.010	2.262 ± 0.077
4 471.68	HeI	-13.365 ± 0.265	2.288 ± 0.265	-12.798 ± 0.001	1.783 ± 0.024
4 634.14	NIII	-13.542 ± 0.624	1.209 ± 0.624	-13.576 ± 0.036	0.695 ± 0.333
4 640.64	NIII	-	-	-13.215 ± 0.013	0.947 ± 0.291
4 685.71	HeII	-12.888 ± 0.464	2.473 ± 0.464	-12.359 ± 0.001	2.106 ± 0.075
4 713.38	HeI*	-13.555 ± 0.549	1.765 ± 0.549	-13.036 ± 0.003	1.419 ± 0.082
4 724.30	[NeIV]	-	-	-14.154 ± 0.057	0.270 ± 0.163
4 740.18	[ArIV]	-13.175 ± 0.206	2.047 ± 0.206	-12.661 ± 0.001	1.813 ± 0.029
4 861.20	Hβ	-11.873 ± 0.212	3.331 ± 0.212	-11.380 ± 0.020	3.032 ± 0.006
4 921.93	HeI	-13.644 ± 0.448	1.442 ± 0.448	-13.180 ± 0.050	1.019 ± 0.063
4 958.52	[OIII]	-11.093 ± 0.187	3.687 ± 0.187	-10.629 ± 0.023	3.270 ± 0.124
5 007.57	[OIII]	-10.646 ± 0.294	3.560 ± 0.294	-10.131 ± 0.017	3.743 ± 0.026
5 191.80	[ArIII]	-	-	-14.152 ± 0.159	0.151 ± 0.004
5 197.90	[NI]	-	-	-13.852 ± 0.019	0.488 ± 0.116
5 411.52	HeII	-13.519 ± 0.094	1.361 ± 0.094	-13.276 ± 0.042	1.107 ± 0.019
5 517.72	[ClIII]	-	-	-14.084 ± 0.025	0.209 ± 0.072
5 537.89	[ClIII]	-13.635 ± 0.005	1.138 ± 0.005	-13.544 ± 0.005	0.801 ± 0.007
5 754.59	[NII]	-12.931 ± 0.048	1.798 ± 0.048	-12.653 ± 0.006	1.650 ± 0.005
5 875.97	HeI	-	-	-11.909 ± 0.024	2.325 ± 0.109
6 300.30	[OI]	-12.638 ± 0.056	2.155 ± 0.056	-12.177 ± 0.026	1.881 ± 0.050
6 312.10	[SIII]	-13.010 ± 0.057	1.868 ± 0.057	-12.606 ± 0.039	1.437 ± 0.011
6 363.77	[OI]	-13.073 ± 0.153	1.756 ± 0.153	-12.656 ± 0.024	1.453 ± 0.038
6 548.05	[NII]	-12.245 ± 0.119	2.398 ± 0.119	-11.733 ± 0.032	1.612 ± 0.116
6 562.85	Hα	-11.024 ± 0.162	3.588 ± 0.162	-10.524 ± 0.002	2.887 ± 0.223
6 583.45	[NII]	-11.781 ± 0.117	2.797 ± 0.117	-11.272 ± 0.008	2.312 ± 0.184
6 678.15	HeI	-12.850 ± 0.008	1.832 ± 0.008	-12.366 ± 0.003	1.743 ± 0.007
6 716.47	[SII]	-13.448 ± 0.042	1.214 ± 0.042	-12.958 ± 0.006	1.151 ± 0.015
6 730.85	[SII]	-13.156 ± 0.155	1.693 ± 0.155	-12.612 ± 0.008	1.495 ± 0.037
7 065.71	HeI	-12.325 ± 0.399	2.461 ± 0.399	-11.860 ± 0.009	2.200 ± 0.044
7 135.80	[ArIII]	-12.097 ± 0.114	2.465 ± 0.114	-	-

in blue spectrum Hβ λ4 861.29, O III λ5 007.57 and O III λ4 959.52.

4 RESULTS AND DISCUSSIONS

The dataset of each PNe is produced by measuring the line flux and their equivalent widths of selected emission lines. In measuring these values, background of each emission line has to be determined and then removed by a first order polynomial fit to the line extending to its wings. The background level of each emission line on the continuum was determined around the line.

The flux values and equivalent widths were then calculated by best fitting to the line. The values and their errors are given in Tables 5–21 which were computed by averaging multiple measurements of Gaussian fits of the same line. The

Table 9. Hu 1-1 fluxes and equivalent widths.

Wavelength Å	Ion	log [Flux] (ergs cm^{-2} s^{-1})	log [EW] (Å)
3 726.19	[OII]	− 11.424 ± 0.002	2.967 ± 0.018
3 797.90	H10	− 13.353 ± 0.011	1.217 ± 0.006
3 835.38	H9	− 13.065 ± 0.006	1.519 ± 0.005
3 868.71	[NeIII]	− 11.768 ± 0.005	2.776 ± 0.094
3 889.05	H8	− 12.524 ± 0.023	2.160 ± 0.142
3 967.41	[NeIII]	− 12.108 ± 0.011	2.727 ± 0.239
4 026.10	HeI*	− 13.547 ± 0.057	1.258 ± 0.007
4 068.91	CII	− 12.929 ± 0.020	1.848 ± 0.064
4 101.74	Hδ	− 12.416 ± 0.008	2.352 ± 0.065
4 340.47	Hγ	− 12.163 ± 0.012	2.607 ± 0.168
4 363.21	[OIII]	− 12.743 ± 0.044	2.027 ± 0.200
4 471.68	HeI	− 13.010 ± 0.084	1.676 ± 0.213
4 640.64	NIII	− 13.518 ± 0.080	1.187 ± 0.058
4 685.71	HeII	− 12.498 ± 0.035	2.677 ± 0.695
4 713.38	HeI*	− 13.574 ± 0.064	2.469 ± 0.048
4 861.20	Hβ	− 11.793 ± 0.001	2.953 ± 0.035
4 921.93	HeI	− 13.408 ± 0.040	1.334 ± 0.068
4 959.52	[OIII]	− 11.179 ± 0.002	3.500 ± 0.186
5 007.57	[OIII]	− 10.734 ± 0.001	3.811 ± 0.158
5 197.90	[NI]	− 13.375 ± 0.159	1.479 ± 0.181
5 411.52	HeII	− 13.449 ± 0.074	1.337 ± 0.099
5 537.89	[CIII]	− 13.109 ± 0.063	1.910 ± 0.286
5 875.97	HeI	− 12.539 ± 0.005	2.346 ± 0.046
6 300.30	[OI]	− 12.378 ± 0.008	2.540 ± 0.014
6 363.77	[OI]	− 12.856 ± 0.008	2.101 ± 0.039
6 562.85	Hα	− 10.912 ± 0.001	1.583 ± 0.002
6 678.15	HeI	− 13.126 ± 0.019	1.763 ± 0.061
6 730.85	[SII]	− 11.911 ± 0.002	2.972 ± 0.050
7 065.71	HeI	− 13.104 ± 0.011	1.826 ± 0.038
7 135.80	[ArIII]	− 12.384 ± 0.003	2.550 ± 0.037

Table 10. M 1-4 fluxes and equivalent widths.

Wavelength Å	Ion	log [Flux] (ergs cm^{-2} s^{-1})	log [EW] (Å)
4 861.20	Hβ	− 12.610 ± 0.087	1.350 ± 0.183
4 959.52	[OIII]	− 11.942 ± 0.021	1.930 ± 0.104
5 007.57	[OIII]	− 11.462 ± 0.007	2.456 ± 0.108
5 875.97	HeI	− 12.845 ± 0.003	1.883 ± 0.013
6 300.30	[OI]	− 14.304 ± 0.056	0.469 ± 0.085
6 312.10	[SIII]	− 13.670 ± 0.011	0.469 ± 0.085
6 562.85	Hα	− 11.443 ± 0.001	3.130 ± 0.056
6 583.45	[NII]	− 12.854 ± 0.022	1.729 ± 0.071
6 678.15	HeI	− 13.292 ± 0.048	1.233 ± 0.086
6 716.47	[SII]	− 13.878 ± 0.015	0.665 ± 0.003
6 730.85	[SII]	− 13.810 ± 0.304	0.714 ± 0.378
7 065.71	HeI	− 12.973 ± 0.054	1.519 ± 0.134
7 135.80	[ArIII]	− 12.820 ± 0.020	1.670 ± 0.063

standard deviation of the fits are then taken as the error values. All the measurements were done using standard tasks of IRAF.

Our values and values of W05 data for PNe: BoBn 1, M 1-5, NGC 6833, and IC 5117 are given in Tables 5–8, respectively. Missing values in the tables are due to the grisms

Table 11. K 3-70 fluxes and equivalent widths.

Wavelength Å	Ion	log [Flux] (ergs cm^{-2} s^{-1})	log [EW] (Å)
4 959.52	[OIII]	− 13.546 ± 0.005	2.871 ± 0.239
5 007.57	[OIII]	− 13.045 ± 0.001	3.276 ± 0.164
5 754.59	[NII]	− 14.256 ± 0.042	2.030 ± 0.309
5 875.97	HeI	− 14.360 ± 0.009	2.125 ± 0.147
6 300.30	[OI]	− 14.815 ± 0.087	1.648 ± 0.135
6 312.10	[SIII]	− 14.994 ± 0.094	1.958 ± 0.653
6 548.05	[NII]	− 13.204 ± 0.001	3.465 ± 0.080
6 562.85	Hα	− 13.130 ± 0.004	3.046 ± 0.289
6 583.45	[NII]	− 12.720 ± 0.002	3.306 ± 0.245
6 678.15	HeI	− 14.903 ± 0.053	1.932 ± 0.486
6 716.47	[SII]	− 14.440 ± 0.051	1.858 ± 0.258
6 730.85	[SII]	− 14.293 ± 0.005	2.160 ± 0.077
7 065.71	HeI	− 14.555 ± 0.045	2.090 ± 0.341
7 135.80	[ArIII]	− 14.139 ± 0.006	2.515 ± 0.204

Table 12. M 1-17 fluxes and equivalent widths.

Wavelength Å	Ion	log [Flux] (ergs cm^{-2} s^{-1})	log [EW] (Å)
4 861.20	Hβ	− 12.734 ± 0.004	3.201 ± 0.391
4 959.52	[OIII]	− 12.014 ± 0.001	3.751 ± 0.415
5 007.57	[OIII]	− 11.511 ± 0.000	4.007 ± 0.211
5 197.90	[NI]	− 14.116 ± 0.098	1.748 ± 0.371
5 754.59	[NII]	− 13.645 ± 0.116	2.026 ± 0.662
5 875.97	HeI	− 13.218 ± 0.013	2.294 ± 0.174
6 300.30	[OI]	− 13.177 ± 0.005	2.361 ± 0.027
6 312.10	[SIII]	− 13.948 ± 0.057	1.609 ± 0.244
6 363.77	[OI]	− 13.601 ± 0.001	1.940 ± 0.001
6 548.05	[NII]	− 12.529 ± 0.000	2.919 ± 0.002
6 562.85	Hα	− 11.948 ± 0.000	3.462 ± 0.001
6 583.45	[NII]	− 12.101 ± 0.004	3.361 ± 0.236
6 678.15	HeI	− 13.813 ± 0.009	1.835 ± 0.460
6 716.47	[SII]	− 13.363 ± 0.004	2.248 ± 0.076
6 730.85	[SII]	− 13.144 ± 0.001	2.486 ± 0.044
7 065.71	HeI	− 13.558 ± 0.011	1.909 ± 0.092
7 135.80	[ArIII]	− 12.968 ± 0.000	2.516 ± 0.002

Table 13. SaSt 2-3 fluxes and equivalent widths.

Wavelength Å	Ion	log [Flux] (ergs cm^{-2} s^{-1})	log [EW] (Å)
4 068.91	CII	− 13.812 ± 0.027	0.701 ± 0.035
4 713.38	HeI*	− 14.145 ± 0.018	0.191 ± 0.022
4 861.20	Hβ	− 12.694 ± 0.001	1.599 ± 0.002
5 007.57	[OIII]	− 14.115 ± 0.002	0.166 ± 0.002
5 754.59	[NII]	− 14.241 ± 0.047	0.007 ± 0.001
6 300.30	[OI]	− 13.715 ± 0.007	0.748 ± 0.015
6 548.05	[NII]	− 12.942 ± 0.002	1.615 ± 0.009
6 562.85	Hα	− 12.114 ± 0.000	2.534 ± 0.003
6 583.45	[NII]	− 12.553 ± 0.001	2.093 ± 0.007
6 716.47	[SII]	− 13.900 ± 0.008	0.684 ± 0.012
6 730.85	[SII]	− 13.723 ± 0.007	0.863 ± 0.008
7 135.80	[ArIII]	− 14.719 ± 0.007	0.783 ± 0.016

Table 14. H 4-1 fluxes and equivalent widths.

Wavelength Å	Ion	log [Flux] (ergs cm^{-2} s^{-1})	log [EW] (Å)
3 712.75	HeII	− 12.403 ± 0.004	2.687 ± 0.093
3 734.37	H13	− 14.359 ± 0.052	0.837 ± 0.053
3 750.15	H12	− 14.125 ± 0.067	1.170 ± 0.158
3 770.63	H11	− 13.918 ± 0.004	1.439 ± 0.007
3 819.70	HeI*	− 13.731 ± 0.016	1.652 ± 0.049
3 835.38	H9	− 13.823 ± 0.008	1.545 ± 0.020
3 868.71	[NeIII]	− 13.226 ± 0.000	2.132 ± 0.003
4 068.91	CIII	− 13.181 ± 0.010	2.329 ± 0.122
4 340.47	Hγ	− 12.954 ± 0.003	2.537 ± 0.060
4 363.21	[OIII]	− 13.698 ± 0.025	1.774 ± 0.109
4 387.93	HeI	− 14.709 ± 0.074	0.809 ± 0.093
4 471.68	HeI	− 13.887 ± 0.042	1.583 ± 0.127
4 685.71	HeII	− 13.567 ± 0.011	2.079 ± 0.091
4 861.20	Hβ	− 12.570 ± 0.000	3.252 ± 0.014
4 921.93	HeI	− 14.177 ± 0.006	1.549 ± 0.014
4 959.52	[OIII]	− 12.247 ± 0.000	3.332 ± 0.014
5 007.57	[OIII]	− 11.773 ± 0.000	3.746 ± 0.099
5 197.90	[NI]	− 14.359 ± 0.052	1.272 ± 0.022
5 411.52	HeII	− 14.525 ± 0.067	1.049 ± 0.017
5 754.59	[NII]	− 14.249 ± 0.005	1.532 ± 0.004
6 300.30	[OI]	− 14.290 ± 0.065	1.308 ± 0.041
6 363.77	[OI]	− 13.950 ± 0.044	1.753 ± 0.169
6 548.05	[NII]	− 13.018 ± 0.153	2.026 ± 0.937
6 562.85	Hα	− 12.060 ± 0.017	3.013 ± 0.858
6 583.45	[NII]	− 12.452 ± 0.010	2.921 ± 0.439
6 678.15	HeI	− 13.875 ± 0.038	1.946 ± 0.226
6 716.47	[SII]	− 14.518 ± 0.029	1.136 ± 0.049
6 730.85	[SII]	− 14.534 ± 0.049	1.119 ± 0.099
7 065.71	HeI	− 13.820 ± 0.011	1.869 ± 0.064
7 135.80	[ArIII]	− 14.634 ± 0.003	1.115 ± 0.007

Table 15. DdDm 1 fluxes and equivalent widths.

Wavelength Å	Ion	log [Flux] (ergs cm^{-2} s^{-1})	log [EW] (Å)
5 875.97	HeI	− 14.549 ± 0.151	2.163 ± 0.247
6 300.30	[OI]	− 14.871 ± 0.069	1.998 ± 0.623
6 312.10	[SIII]	− 15.104 ± 0.109	1.508 ± 0.414
6 548.05	[NII]	− 13.346 ± 0.002	3.233 ± 0.303
6 562.85	Hα	− 13.247 ± 0.001	3.258 ± 0.278
6 583.45	[NII]	− 12.847 ± 0.000	3.668 ± 0.229
6 678.15	HeI	− 15.090 ± 0.027	1.697 ± 0.192
6 716.47	[SII]	− 14.480 ± 0.001	2.499 ± 0.046
6 730.85	[SII]	− 14.331 ± 0.006	2.458 ± 0.265
7 065.71	HeI	− 14.736 ± 0.017	2.693 ± 0.841
7 135.80	[ArIII]	− 14.245 ± 0.002	3.372 ± 0.627

having different wavelength coverages. For PNe DdDm 1, however, due to having no overlapping wavelength coverage it is excluded in Table 15. Note that, He I lines are double blended in all data sets.

The corresponding error values of the data given in Tables 5–21 are around ±0.03 dex with a standard deviation of ±0.003 dex. To get an impression of the error budget, percentages of flux-to-error ratios are summed over both for all the emission lines and for five bright emission lines, and they are listed in Table 2.

Table 16. Na 1 fluxes and equivalent widths.

Wavelength Å	Ion	log [Flux] (ergs cm^{-2} s^{-1})	log [EW] (Å)
3 726.19	[OII]	− 13.408 ± 0.053	1.270 ± 0.078
3 868.71	[NeIII]	− 12.329 ± 0.004	2.348 ± 0.038
3 889.05	H8	− 13.090 ± 0.033	1.551 ± 0.074
3 967.41	[NeIII]	− 12.681 ± 0.011	2.081 ± 0.066
4 101.74	Hδ	− 12.908 ± 0.017	1.895 ± 0.060
4 340.47	Hγ	− 12.660 ± 0.001	2.135 ± 0.002
4 363.21	[OIII]	− 13.133 ± 0.019	1.667 ± 0.056
4 471.68	HeI	− 13.481 ± 0.168	1.396 ± 0.286
4 640.64	NIII	− 13.409 ± 0.004	1.526 ± 0.000
4 685.71	HeII	− 12.997 ± 0.019	1.849 ± 0.072
4 713.38	HeI*	− 13.479 ± 0.076	1.353 ± 0.141
4 740.18	[ArIV]	− 13.602 ± 0.112	1.242 ± 0.180
4 861.20	Hβ	− 12.175 ± 0.003	2.759 ± 0.062
4 959.52	[OIII]	− 11.497 ± 0.001	3.216 ± 0.071
5 007.57	[OIII]	− 11.014 ± 0.001	3.659 ± 0.178
5 197.90	[NII]	− 14.205 ± 0.520	0.708 ± 0.585
5 411.52	HeII	− 13.913 ± 0.005	0.920 ± 0.006
5 875.97	HeI	− 12.692 ± 0.001	2.113 ± 0.006
6 300.30	[OI]	− 14.600 ± 0.118	0.332 ± 0.146
6 312.10	[SIII]	− 14.048 ± 0.014	0.832 ± 0.012
6 562.85	Hα	− 11.419 ± 0.000	3.417 ± 0.024
6 583.45	[NII]	− 13.347 ± 0.045	1.477 ± 0.079
6 678.15	HeI	− 13.235 ± 0.020	1.626 ± 0.056
6 730.85	[SII]	− 13.748 ± 0.061	1.136 ± 0.085
7 065.71	HeI	− 13.227 ± 0.004	1.639 ± 0.013
7 135.80	[ArIII]	− 13.013 ± 0.003	1.858 ± 0.011

Number of lines detected for each object varied between 11 and 35 amounting to 375 emission lines for all objects. In addition to this in total 49 *different* emission lines were identified where they were mostly caused by collisions (Kwok 2000, p. 260) or they were the recombination lines of H I, He I and He II. However, a considerable amount of recombination lines of heavy elements were also detected such as O I, O II, O III, C IV, and Ne III. In some of the sources (BoBn 1, K 3-70, DdDm 1, and M 1-4) emission lines were observed on an elevated continuum level which was due to the recombination of electrons.

Among 49 emission lines, the brightest (unsaturated) and faintest ones were the O III λ5 007.57 with −9.947 ± 0.002 from IC 4997, and N II λ6 548.05 with −15.115 ± 0.080 from M 1–5, respectively. Emission line fluxes of PNe are directly proportional with optical R magnitude of the source (see Table 1) which was also noted in this work (see Tables 5–21).

Observed Hβ fluxes were compared with A92 and plotted in top panel of Figure 3 (17 in total). As can be deduced from the plot, an obvious linear relation exists for both

Table 17. Vy 1-2 fluxes and equivalent widths.

Wavelength Å	Ion	log [Flux] (ergs cm^{-2} s^{-1})	log [EW] (Å)
3 750.15	H12	− 12.118 ± 0.011	1.832 ± 0.043
3 797.90	H10	− 12.631 ± 0.001	1.567 ± 0.048
3 819.70	He I*	− 12.895 ± 0.036	1.420 ± 0.095
3 868.71	[Ne III]	− 12.795 ± 0.010	1.417 ± 0.029
3 889.05	H8	− 11.578 ± 0.003	2.655 ± 0.014
4 026.10	He I*	− 13.224 ± 0.010	1.198 ± 0.018
4 068.91	C III	− 13.000 ± 0.020	1.396 ± 0.034
4 101.74	Hδ	− 12.120 ± 0.007	2.313 ± 0.069
4 340.47	Hγ	− 11.928 ± 0.002	2.496 ± 0.025
4 363.21	[O III]	− 12.638 ± 0.007	1.766 ± 0.013
4 471.68	He I	− 12.938 ± 0.060	1.551 ± 0.162
4 634.14	N III	− 12.767 ± 0.069	1.721 ± 0.171
4 685.71	He II	− 12.101 ± 0.008	2.341 ± 0.107
4 713.38	He I*	− 12.926 ± 0.082	1.532 ± 0.217
4 740.18	[Ar IV]	− 12.992 ± 0.061	1.497 ± 0.163
4 861.20	Hβ	− 11.552 ± 0.005	2.981 ± 0.215
4 921.93	He I	− 12.860 ± 0.007	1.754 ± 0.003
4 959.52	[O III]	− 11.052 ± 0.003	3.369 ± 0.241
5 007.57	[O III]	− 10.700 ± 0.002	3.711 ± 0.253
5 411.52	He II	− 13.088 ± 0.019	1.679 ± 0.055
5 875.97	He I	− 12.326 ± 0.014	2.466 ± 0.160
6 300.30	[O I]	− 13.238 ± 0.057	1.547 ± 0.082
6 312.10	[S III]	− 13.242 ± 0.028	1.641 ± 0.191
6 363.77	[O I]	− 13.685 ± 0.016	1.080 ± 0.027
6 548.05	[N II]	− 12.576 ± 0.045	2.071 ± 0.008
6 562.85	Hα	− 11.201 ± 0.000	3.496 ± 0.121
6 583.45	[N II]	− 12.147 ± 0.005	2.630 ± 0.114
6 678.15	He I	− 12.973 ± 0.006	1.808 ± 0.026
6 716.47	[S II]	− 13.163 ± 0.023	1.634 ± 0.066
6 730.85	[S II]	− 12.954 ± 0.003	1.820 ± 0.011
7 065.71	He I	− 12.973 ± 0.001	1.823 ± 0.007
7135.80	[Ar III]	− 12.394 ± 0.002	2.384 ± 0.021

Table 18. M 3-27 fluxes and equivalent widths.

Wavelength Å	Ion	log [Flux] (ergs cm^{-2} s^{-1})	log [EW] (Å)
3 770.63	H11	− 12.014 ± 0.003	2.182 ± 0.023
3 797.90	H10	− 12.964 ± 0.038	1.222 ± 0.066
3 967.41	[Ne III]	− 13.296 ± 0.013	0.926 ± 0.019
4 026.10	He I*	− 13.161 ± 0.055	1.090 ± 0.076
4 068.91	C III	− 12.760 ± 0.014	1.479 ± 0.033
4 340.47	Hγ	− 12.513 ± 0.023	1.761 ± 0.086
4 363.21	[O III]	− 12.031 ± 0.011	2.251 ± 0.098
4 471.68	He I	− 12.978 ± 0.056	1.320 ± 0.107
4 713.38	He I*	− 13.521 ± 0.138	0.753 ± 0.168
4 861.20	Hβ	− 11.930 ± 0.004	2.353 ± 0.041
4 921.93	He I	− 13.377 ± 0.040	0.946 ± 0.054
5 875.97	He I	− 12.186 ± 0.014	2.164 ± 0.146
6 300.30	[O I]	− 12.471 ± 0.001	1.845 ± 0.031
6 312.10	[S III]	− 12.841 ± 0.013	1.634 ± 0.001
6 363.77	[O I]	− 12.710 ± 0.035	1.685 ± 0.117
6 548.05	[N II]	− 10.958 ± 0.002	2.395 ± 0.015
6 562.85	Hα	− 10.607 ± 0.001	3.417 ± 0.160
6 678.15	He I	− 12.887 ± 0.049	1.328 ± 0.121
6 730.85	[S II]	− 12.671 ± 0.097	0.729 ± 0.111
7 065.71	He I	− 12.195 ± 0.003	2.083 ± 0.024
7 135.80	[Ar III]	− 12.997 ± 0.047	1.339 ± 0.117

bright and faint flux arms with a R^2 value 0.89 on the faint arm.

A similar comparison was done for W05 including all emission lines (64 in total). However, only 4 PNe (BoBn 1, IC 5117, M 1-5, and NGC 6833) were used in the comparison (see Tables 5–8). The comparisons for flux and EW values are shown in middle and bottom panels of Figure 3, respectively. Corresponding R^2 values of flux and EW are 0.96 and 0.88, respectively. The deviations seen in the regression are mainly due to not resolving the faint lines.

In comparing our values with W05, there are some discrepancies which have to be mentioned in detail. The error in flux measurement of each emission line (Table 2) amounts to less than 1% of the line strength. On top of this, low SNR of the spectra on relatively bad seeing conditions produced slit losses which accumulated to no more than 10% of the signal, therefore causing a relatively low flux value. However, in the absence of these negative effects a high consistency is achieved in the comparison which makes the results on the whole reliable.

Physical and chemical properties for all PNe having suitable data sets were also calculated. The analysis of the data was based on Corradi et al. (1997). Since the Balmer decrement is a sign of extinction along the observed column of ISM, extinction constant (c_β) were calculated using H α/H β ratio. Electron temperatures (T_e) and densities (N_e) were calculated using IRAF's nebular.temden task. Electron temperatures of T_e([O III]) and T_e([N II]) were calculated according to Osterbrock & Ferland (2006). Using ratio of [S II]λ6716/λ6731 and assuming an electron temperature of $T = 10^4$ K, electron densities were calculated. All above calculations are given in Table 3.

For each PNe, the ionic abundances relative to Hydrogen are computed from the line fluxes relative to Hβ using the temperatures and densities values given in Table 3 (see e.g. Kingsburgh & Barlow 1994; Wesson, Liu, & Barlow 2005 for computation methods). These abundances are given in Table 4.

In calculating the values of Table 4, de-reddened fluxes have been used according to Acker (2011). In addition to this, excitation class of each PNe was also calculated according to Gurzadian & Egikian (1991) in which the nebular lines have been used as a (loosely) measure of the temperature of the central white dwarf. Note that, if the stellar nuclei of the PNe is found to be very hot then it can be taken as a *high excitation PNe*. Therefore, Hu 1-1, BoBn 1, and Vy 1-2 fall into this category. However, if some related lines are missing from the central region then a definitive calculation could not be made. Therefore the following PNe fall into this *unidentified*

Table 19. IC 4997 fluxes and equivalent widths.

Wavelength Å	Ion	log [Flux] (ergs cm^{-2} s^{-1})	log [EW] (Å)
3 734.37	H13	− 11.186 ± 0.057	2.102 ± 0.307
3 770.63	H11	− 12.230 ± 0.080	1.051 ± 0.161
3 797.90	H10	− 11.917 ± 0.053	1.364 ± 0.137
3 819.70	He I*	− 11.788 ± 0.026	1.508 ± 0.085
3 835.38	H9	− 12.395 ± 0.120	0.882 ± 0.188
3 868.71	[Ne III]	− 10.466 ± 0.002	2.813 ± 0.079
3 889.05	H8	− 11.290 ± 0.013	1.968 ± 0.101
3 967.41	[Ne III]	− 10.790 ± 0.002	2.450 ± 0.039
4 026.10	He I*	− 12.143 ± 0.039	1.109 ± 0.080
4 068.91	C III	− 11.959 ± 0.064	1.338 ± 0.124
4 101.74	Hδ	− 11.105 ± 0.007	2.182 ± 0.080
4 340.47	Hγ	− 10.878 ± 0.001	2.419 ± 0.028
4 363.21	[O III]	− 10.822 ± 0.004	2.468 ± 0.095
4 387.93	He I	− 12.580 ± 0.010	0.872 ± 0.001
4 471.68	He I	− 11.770 ± 0.015	1.603 ± 0.060
4 640.64	N III	− 12.296 ± 0.071	1.120 ± 0.003
4 713.38	He I*	− 12.384 ± 0.016	0.999 ± 0.030
4 740.18	[Ar IV]	− 12.571 ± 0.274	0.883 ± 0.366
4 861.20	Hβ	− 10.587 ± 0.002	2.742 ± 0.066
4 921.93	He I	− 12.309 ± 0.057	1.049 ± 0.100
4 959.52	[O III]	− 10.342 ± 0.002	2.959 ± 0.090
5 007.57	[O III]	− 9.947 ± 0.002	3.306 ± 0.190
5 754.59	[N II]	− 12.380 ± 0.008	1.156 ± 0.017
5 875.97	He I	− 11.122 ± 0.004	2.393 ± 0.051
6 300.30	[O I]	− 11.638 ± 0.011	1.874 ± 0.067
6 312.10	[S III]	− 11.937 ± 0.010	1.561 ± 0.063
6 363.77	[O I]	− 12.103 ± 0.004	1.348 ± 0.010
6 548.05	[N II]	− 11.451 ± 0.010	1.912 ± 0.069
6 562.85	Hα	− 10.038 ± 0.000	3.315 ± 0.064
6 583.45	[N II]	− 11.050 ± 0.006	2.294 ± 0.087
6 678.15	He I	− 11.714 ± 0.008	1.749 ± 0.049
6 716.47	[S II]	− 12.464 ± 0.059	1.002 ± 0.103
6 730.85	[S II]	− 12.176 ± 0.007	1.273 ± 0.017
7 065.71	He I	− 11.229 ± 0.002	2.239 ± 0.037
7 135.80	[Ar III]	− 11.343 ± 0.001	2.123 ± 0.019

Table 20. Me 2-2 fluxes and equivalent widths.

Wavelength Å	Ion	log [Flux] (ergs cm^{-2} s^{-1})	log [EW] (Å)
3 734.37	H13	− 11.865 ± 0.002	1.839 ± 0.007
3 770.63	H11	− 12.898 ± 0.033	0.881 ± 0.060
3 819.70	He I*	− 12.579 ± 0.031	1.280 ± 0.071
3 835.38	H9	− 12.990 ± 0.104	0.887 ± 0.159
3 868.71	[Ne III]	− 11.402 ± 0.002	2.492 ± 0.033
3 889.05	H8	− 11.958 ± 0.002	1.946 ± 0.036
3 967.41	[Ne III]	− 11.688 ± 0.003	2.259 ± 0.037
4 026.10	He I*	− 12.668 ± 0.013	1.289 ± 0.032
4 101.74	Hδ	− 11.796 ± 0.003	2.145 ± 0.034
4 340.47	Hγ	− 11.555 ± 0.003	2.432 ± 0.056
4 363.21	[O III]	− 12.438 ± 0.023	1.547 ± 0.079
4 387.93	He I	− 13.299 ± 0.150	0.730 ± 0.185
4 471.68	He I	− 12.308 ± 0.031	1.804 ± 0.165
4 713.38	He I*	− 12.974 ± 0.034	1.089 ± 0.060
4 740.18	[Ar IV]	− 13.405 ± 0.015	0.686 ± 0.015
4 861.20	Hβ	− 11.163 ± 0.002	2.885 ± 0.093
4 921.93	He I	− 12.845 ± 0.020	1.201 ± 0.039
4 959.52	[O III]	− 10.778 ± 0.007	3.196 ± 0.040
5 007.57	[O III]	− 10.323 ± 0.001	3.600 ± 0.043
5 191.80	[Ar III]	− 13.212 ± 0.100	0.948 ± 0.152
5 537.89	[Cl III]	− 13.483 ± 0.007	0.725 ± 0.003
5 754.59	[N II]	− 13.811 ± 0.014	0.368 ± 0.003
5 875.97	He I	− 11.650 ± 0.004	2.472 ± 0.091
6 300.30	[O I]	− 12.688 ± 0.021	1.511 ± 0.071
6 312.10	[S III]	− 13.190 ± 0.117	0.977 ± 0.208
6 363.77	[O I]	− 13.103 ± 0.051	1.119 ± 0.102
6 548.05	[N II]	− 11.350 ± 0.004	2.719 ± 0.160
6 562.85	Hα	− 10.590 ± 0.001	3.489 ± 0.182
6 583.45	[N II]	− 10.860 ± 0.002	3.296 ± 0.082
6 678.15	He I	− 12.280 ± 0.005	1.896 ± 0.057
6 716.47	[S II]	− 13.236 ± 0.001	1.024 ± 0.002
6 730.85	[S II]	− 13.116 ± 0.031	1.094 ± 0.051
7 065.71	He I	− 11.831 ± 0.003	2.354 ± 0.057
7 135.80	[Ar III]	− 12.056 ± 0.006	2.128 ± 0.076

Table 21. Vy 2-3 fluxes and equivalent widths.

Wavelength Å	Ion	log [Flux] (ergs cm^{-2} s^{-1})	log [EW] (Å)
3 750.15	H12	− 12.104 ± 0.010	1.733 ± 0.025
3 889.05	H8	− 12.559 ± 0.013	1.317 ± 0.025
4 068.91	C III	− 12.630 ± 0.012	1.270 ± 0.020
4 340.47	Hγ	− 12.393 ± 0.003	1.576 ± 0.006
4 363.21	[O III]	− 13.169 ± 0.020	0.803 ± 0.025
4 471.68	He I	− 13.326 ± 0.080	0.659 ± 0.094
4 685.71	He II	− 13.776 ± 0.073	0.222 ± 0.079
4 713.38	He I*	− 13.707 ± 0.034	0.300 ± 0.037
4 861.20	Hβ	− 11.997 ± 0.002	2.047 ± 0.012
4 959.52	[O III]	− 11.486 ± 0.001	2.562 ± 0.016
5 007.57	[O III]	− 11.053 ± 0.000	2.993 ± 0.010
5 875.97	He I	− 12.686 ± 0.016	1.568 ± 0.043
6 562.85	Hα	− 11.436 ± 0.001	2.938 ± 0.027
6 583.45	[N II]	− 13.527 ± 0.009	0.865 ± 0.017
6 678.15	He I	− 13.252 ± 0.011	1.179 ± 0.019
7 065.71	He I	− 13.328 ± 0.015	1.168 ± 0.025
7 135.80	[Ar III]	− 12.980 ± 0.003	1.520 ± 0.008

category: M 1-4, K 3-70, M1-17 SaSt 2-3, DdDm 1 M 3-27, IC 4997, and Me 2-2. Finally, the rest of the PNe can safely be classified as *medium excitation PNe*.

These studies can significantly contribute to the study of the evolution of the PNe and the Galaxy.

5 CONCLUSIONS

- A similar study of D97 (for southern Hemisphere) and W05 (for northern Hemisphere) have been carried out by extending the northern hemisphere coverage of PNe.
- We present new emission line fluxes to be used as a standard in both imaging in narrow band and in Fabry–Perot spectroscopy.
- Emission line flux measurements of 12 PNe were made for the first time.
- Physical and chemical properties of PNe, as well as their evolution, can be studied with continuous monitoring of these 17 PNe.

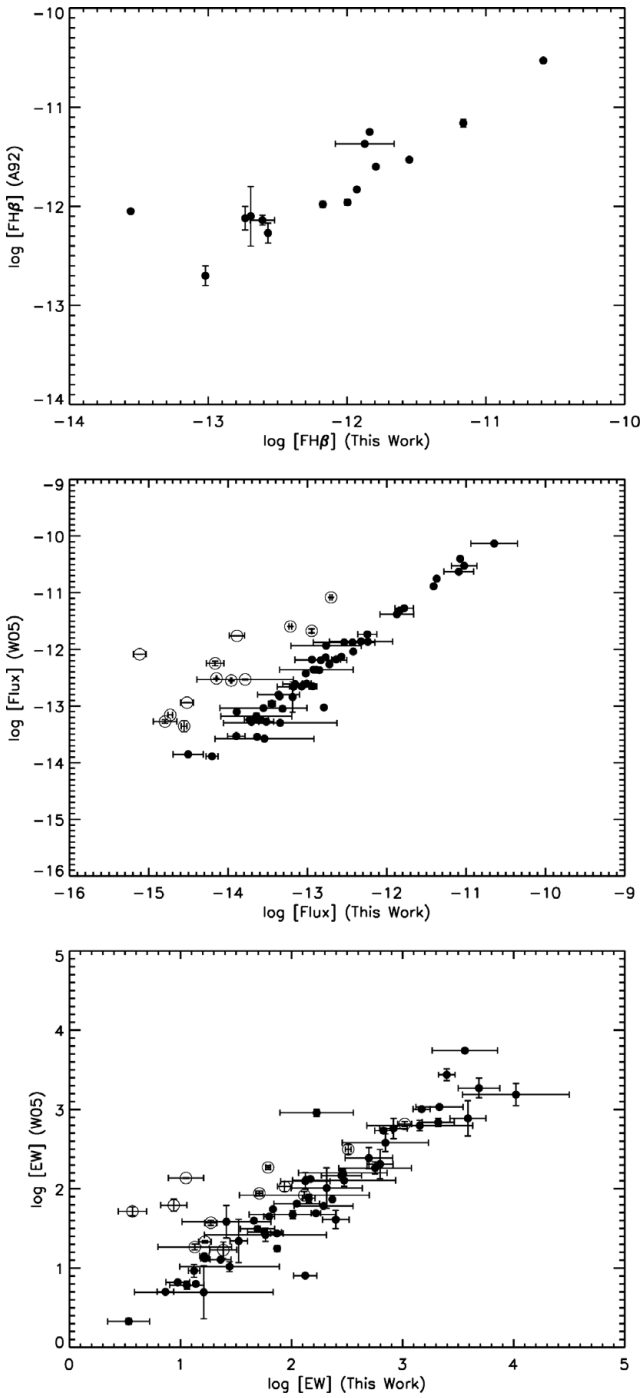

Figure 3. In the top panel a comparison of Hβ fluxes of A92 (vertical) with this work (horizontal) is given. In the middle and bottom panels, a comparison of all emission line fluxes (in total 64 for 4 PNe) and EW of W05 (vertical) with this work (horizontal) are given, respectively. Open circles represent faint and blended He I lines. All axes are in log scale and fluxes are in *ergs* $cm^2 s^{-1}$.

- For suitable PNe, extinction constant, electron temperature, electron density, chemical abundance, and excitation class have been calculated.

ACKNOWLEDGEMENTS

The authors thank to the scientific and technological research council of Turkey (TUBITAK) for a partial support in using RTT150 (Russian–Turkish 1.5-m telescope) in Antalya through with project numbers 10BRTT150-33-0 and 10ARTT150-489-0. NA also thank to TUBITAK National Observatory (TUG) staff. NA gratefully acknowledges support through a Post-Doc Fellowship from the TUBITAK-BIDEB at Physics Department of Middle East Technical University, Ankara–Turkey. The author also grateful to M. E. Ozel for reading and correcting the manuscript and for his valuable remarks.

REFERENCES

Acker, A. 2011, in EAS Publications Series, ed. J. -P. Rozelot, & C. Neiner (Vol. 47), 189–214
Acker, A., Marcout, J., Ochsenbein, F., Stenholm, B., Tylenda, R., & Schohn, C. 1992, The Strasbourg-ESO Catalogue of Galactic Planetary Nebulae. Parts I, II. European Southern Observatory, Garching, Germany
Baldwin, J. A., & Stone, R. P. S. 1984, MNRAS, 206, 241
Corradi, R. L. M., Perinotto, M., Schwarz, H. E., & Claeskens, J. -F. 1997, A&A, 322, 975
Dopita, M. A., & Hua, C. T. 1997, ApJS, 108, 515
Gurzadian, G. A., & Egikian, A. G. 1991, Ap&SS, 181, 73
Johnson, H. L., & Harris, D. L. 1954, ApJ, 120, 196
Kingsburgh, R. L., & Barlow, M. J. 1994, MNRAS, 271, 257
Kwok, S. 2000, The Origin and Evolution of Planetary Nebulae/Sun Kwok, Cambridge Astrophysics Series (Vol. 33; Cambridge: Cambridge University Press), 260
Landolt, A. U. 1992, AJ, 104, 340
Liller, W. 1955, ApJ, 122, 240
Madsen, G. J., Frew, D. J., Parker, Q. A., Reynolds, R. J., & Haffner, L. M. 2006, An Optical Emission Line Survey of Large Planetary Nebulae, in IAU Symposium, Vol. 234, Planetary Nebulae in our Galaxy and Beyond, ed. M. J. Barlow, & R. H. Méndez (Cambridge: Cambridge University Press), 455
Massey, P., Strobel, K., Barnes, J. V., & Anderson, E. 1988, ApJ, 328, 315
O'Dell, C. R. 1963, ApJ, 138, 1018
Oke, J. B. 1990, AJ, 99, 1621
Osterbrock, D. E., & Ferland, G. J. 2006, Astrophysics of gaseous nebulae and active galactic nuclei (Sausalito, CA: University Science Books)
Ozisik, T., & Ak, T. 2004, A&A, 422, 1129
Stone, R. P. S., & Baldwin, J. A. 1983, MNRAS, 204, 347
Wesson, R., Liu, X.-W., & Barlow, M. J. 2005, MNRAS, 362, 424
Wright, S. A., Corradi, R. L. M., & Perinotto, M. 2005, A&A, 436, 967